Vapor phase selective hydrogenation of furfural to furfuryl alcohol over Cu–MgO coprecipitated catalysts

B.M. Nagaraja, A.H. Padmasri, B. David Raju, K.S. Rama Rao [*]

Inorganic & Physical Chemistry Division, Indian Institute of Chemical Technology, Tarnaka, Hyderabad 500007, India

Abstract

Cu–MgO catalysts have been employed for the catalytic vapor phase hydrogenation of furfural (FAL) to furfuryl alcohol (FOL) at atmospheric pressure, H_2/furfural (molar ratio) = 2.5 and the gas hourly space velocity (GHSV) has been maintained at $0.05 \, mol \, h^{-1} \, g \, cat^{-1}$. Cu–MgO catalysts with variable Cu loadings (5.2–79.8 wt.%) are prepared by coprecipitation method and are characterized by BET surface area, AAS (atomic adsorption spectroscopy), XRD, XPS and DTA/TGA. Hydrogenation activities of the catalysts, reduced at 523 K in H_2 flow for 4 h prior to the reaction are studied in the temperature range of 453–523 K. Cu–MgO catalyst with 16 wt.% of Cu showed hydrogenation activity with 98% conversion of furfural producing furfuryl alcohol with a higher selectivity of 98%. XPS analysis showed the presence of Cu^0/Cu^+ sites on the catalyst surface that may be responsible for the higher activity compared to other Cu–MgO catalysts studied. The turnover frequency of furfural conversion in the catalysts containing lower composition of Cu is very high. However, due to the lack of required number of Cu^0 particles and the absence of Cu^+ species in these catalysts, the overall conversion of furfural is low.
© 2006 Elsevier B.V. All rights reserved.

Keywords: Hydrogenation; Furfural; Furfuryl alcohol; Coprecipitation method; Cu–MgO catalyst; Loading effect; Temperature effect

1. Introduction

Furfuryl alcohol (2-furan methanol) is an important chemical in polymer industry [1,2]. It is used mainly for the production of thermostatic resins, liquid resins used for strengthening ceramics. Furfuryl alcohol is also used in producing various synthetic fibers, rubber-resins and farm chemical [3,4]. It is an important chemical intermediate for the manufacture of lysine, Vitamin C, lubricant, dispersing agent and plasticizer. The hydrogenation of furfural (FAL) to furfuryl alcohol (FOL) is carried out either in the gas phase or in the liquid phase [5–8]. The catalyst mainly used for FAL hydrogenation in the industry is a Cu–Cr catalyst modified with various promoters [5]. The toxicity in Cu–Cr catalysts due to the presence of Cr_2O_3 cause severe environmental pollution. Application of Raney Ni; Raney Co and Raney Cu in the FAL hydrogenation have also been reported; but these catalysts show low activity or/and low selectivity [9].

Recently, a few works concerning the hydrogenation of furfural over heterogeneous catalysts have been published.

Some of these are carbon-supported copper, Raney Ni, Nickel amorphous alloy and mixed copper zinc oxides with Al, Mn, and Fe [3,6,10–13]. Homogeneous complexes of Ru, Rh and Pt are also reported as active catalysts for the synthesis of furfuryl alcohol [14].

In our earlier communication, hydrogenation of furfural to furfuryl alcohol is studied over Cu–MgO catalysts prepared by coprecipitation, impregnation and solid-solid wetting methods [15]. It has been observed that the catalyst prepared by coprecipitation method gave a higher conversion and higher selectivity towards the formation of FOL, than other catalysts.

The present work is a detailed study dealing with the effect of Cu loading on the hydrogenation of furfural over coprecipitated Cu–MgO catalysts. All the catalysts have been well characterized by BET surface area, AAS (Atomic adsorption spectroscopy), DTA/TG, XRD and XPS. The hydrogenation activities of these catalysts have been correlated with the physico-chemical properties, wherever possible.

2. Experimental

Cu–MgO catalysts with Cu loadings of 5.2, 10.1, 13.5, 16, 37.3, 42.9, 51.6 and 79.8% (in wt.%) are prepared by

---

coprecipitation method and designated as CM1, CM2, CM3, CM4, CM5, CM6, CM7 and CM8. Aqueous solution of 1 M each of $Cu(NO_3)_2 \cdot 3H_2O$ (M/S. Loba Chemie, India) and $Mg(NO_3)_2 \cdot 6H_2O$ (M/S. Loba Chemie, India) are mixed together. The mixed solution is precipitated at pH 9.0 by a slow addition of 1 M aqueous solution of K_2CO_3 (M/S. Loba Chemie, India). The precipitate is filtered and washed three times with 500 ml of distilled H_2O and dried at 393 K for 12 h. The dried sample is then calcined in air at 723 K for 4 h and reduced in H_2 flow at 523 K for 4 h prior activity study. The bulk CuO catalyst used for comparison of the activity with Cu–MgO catalyst is also prepared in a similar way using K_2CO_3 as the precipitating agent.

XRD patterns are recorded using a Siemens D-5000 diffractometer with Ni filtered Cu Kα as a radiation source. Kratos axis 165 XPS spectrometer, with Mg Kα radiation (1253.6 eV), has been used for obtaining ESCA data. In the ESCA study, C1s binding energy value of 285 eV is used as a reference and the relative atomic sensitivity factors of 4.871 and 0.168 for $Cu2p_{3/2}$ and $Mg2p$, respectively, have been chosen for determining Cu/Mg surface compositions of reduced Cu–MgO samples.

DTA/TGA profiles of Cu–MgO samples (in dried form) are recorded on a Metler Toledo 851E (Switzerland) instrument at a heating rate of 10 K min^{-1} in air from 298 to 1273 K.

Vapor phase hydrogenation of furfural has been carried out in a fixed bed quartz reactor (200 mm long and 8 mm i.d.). About 1 g of catalyst packed at the center of reactor between two plugs of quartz wool has been reduced in a flow of 6% H_2 in He mixture at 523 K for 4 h followed by lowering the temperature of the reactor to 453 K and replacing the H_2/He mixture with ultra pure H_2 (99.9% H_2 which is further purified by passing through de-oxo and molecular sieve traps kept in series to remove oxygen and moisture, respectively). Furfural (1.2 ml/h) is injected with the help of a syringe pump (Secura FT, B. Braun Germany) with H_2/furfural (molar ratio = 2.5). H_2 flow has been monitored using rotameter. Gas hourly space velocity (GHSV) has been maintained at 0.05 mol h^{-1} g cat^{-1}. The product mixture was collected every hour in an ice-cold trap and analyzed by a GC–MS (QP-5050, M/S. Shimadzu instruments, Japan) using a DB-5MS capillary column of 0.32 mm dia. and 25 m long (M/S. J&W Scientific Instruments, USA).

3. Results and discussion

3.1. BET-surface area and XRD results

Table 1 presents the BET-surface areas and the crystalline phases of different Cu–MgO coprecipitated catalysts both in calcined and reduced form. The surface area of MgO is found to be 38 m^2 g^{-1} and the surface area of the Cu–MgO coprecipitated catalysts are lower in low loadings of Cu compared to MgO. This indicates that addition of Cu to MgO reduced the surface areas of the support MgO probably due to the coverage of the MgO surface by Cu initially. The BET surface area started increasing with increase in Cu loading and reaches a maximum of 46 m^2 g^{-1} at a Cu loading of 16 wt.% and thereafter reduced with further increase in the Cu content probably due to the formation of larger crystallites of CuO. The growth in the intensity of CuO diffraction lines is observed with the increase in Cu loading from 5.2 to 79.8 wt.%. The calcined catalysts with lower loadings of Cu from 5.2 to 13.5 wt.% showed only a poorly crystalline MgO phase and very poorly marked d lines of CuO. The reduced catalysts have shown the presence of CuO phase in lower Cu loadings. In the catalysts CM3, CM4, CM7 and CM8, crystalline phases due to Cu^0, Cu^+, and Cu^{++} oxides are present. However, at higher loadings i.e., in CM7 and CM8, the intensity of d lines of Cu^0 phase reduces at the expense of CuO and Cu_2O phases. This may be due to an incomplete reduction of the bulk CuO or due to re-oxidation of the Cu^0 species to Cu^+ and Cu^{2+} formed at higher loadings of Cu. In CM5 and CM6, only Cu^0 species are present. The used catalysts (after the reaction) indicated an increase in the intensity of CuO phase with increase in Cu loading (Cu loading $\geq$ 37.3 wt.%) and the presence of Cu^0 phase is much clear in all the used samples, collected after the reduction. In the samples of higher Cu loadings where bulky nature of CuO species are present, both Cu metallic and Cu^{++} species are visible. In the lower Cu loading containing used catalysts, the interaction between Cu and MgO and the smaller crystallite size of Cu maintains Cu^0 species.

The X-ray line broadening analysis clearly showed an increase in the crystallite size of Cu with the increase in the loading of Cu as depicted in Fig. 1. The increase in the crystallite size of Cu may be attributed to the agglomerization of Cu particles with increase in Cu content. However, the N$_2$O titration

Table 1
Physical characteristics of Cu-catalysts

Catalyst	Cu[a] (wt.%)	BET-surface area (m^2 g^{-1})[b]	XRD phases		
			Calcined	Reduced	Used
CM1	5.2	19	CuO, MgO	CuO, MgO	Cu^0, MgO
CM2	10.1	25	CuO, MgO	CuO, MgO	Cu^0, MgO
CM3	13.5	34	CuO, MgO	Cu^0, Cu_2O, CuO, MgO	Cu^0, MgO
CM4	16.0	46	CuO, MgO	Cu^0, Cu_2O, CuO, MgO	Cu^0, MgO
CM5	37.3	38	CuO, MgO	Cu^0, MgO	Cu^0, CuO, MgO
CM6	42.9	28	CuO, MgO	Cu^0, MgO	Cu^0, CuO, MgO
CM7	51.6	25	CuO, MgO	Cu^0, Cu_2O, CuO, MgO	Cu^0, CuO, MgO
CM8	79.8	20	CuO, MgO	Cu^0, Cu_2O, CuO, MgO	Cu^0, CuO, MgO

[a] Obtained from AAS analysis.
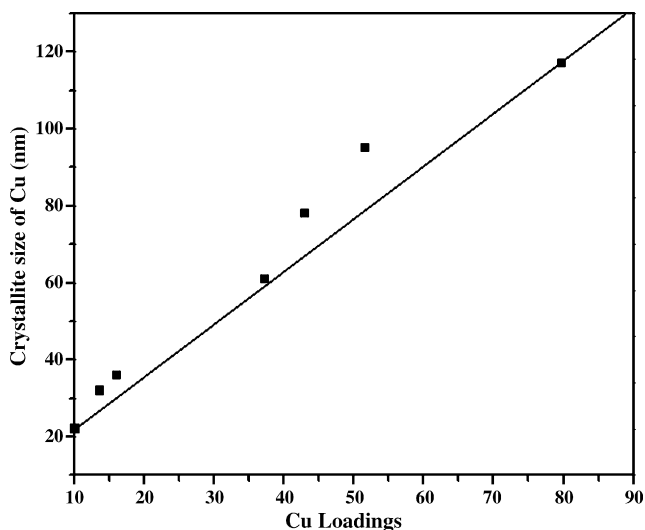
[b] Of calcined sample.

Fig. 1. Variation in the crystallite size of Cu with Cu-loading in Cu–MgO catalysts.

results from our previous studies over the Cu–MgO coprecipitated catalysts have shown an increase in dispersion of Cu with loading upto 16 wt.%. (CM4) and thereafter a fall in the dispersion of Cu loading to the formation bigger particles of Cu [16].

3.2. XPS discussion

The catalysts have been characterized by X-ray photoelectron spectroscopy to obtain more information about the Cu oxidation state and the chemical compositions in the samples. XPS analysis of Cu–MgO catalysts prepared by different methods has been reported in our earlier work where it has been shown that a large amount of Cu^0 species are present at the surface in the coprecipitated catalysts as compared to the catalysts prepared by impregnation and solid-solid wetting methods [15]. Cu2p XPS spectra of various Cu–MgO coprecipitated and reduced catalysts with varying Cu contents are shown in Fig. 2. All the catalysts show the presence of $Cu2p_{3/2}$ peak in the range of 933–934 eV. Although the XRD patterns clearly indicate the presence of Cu^0 formation in the catalysts with low Cu contents, the XPS data, however, shows the presence of CuO in all the samples. But from XRD results it is clear that Cu^0 species are present in higher

concentrations than that of CuO. A clear separation of peaks corresponding to Cu^0 and CuO is not observed in the XPS spectra. However, Carley et al. have ascribed a peak at 933.4 eV to Cu^0 for the Cu/Al_2O_3 catalysts and corresponding to smaller particles of Cu^0 with a surface coverage of 6×10^3 atom cm^{-2} [17]. The Cu–MgO catalysts of high Cu concentrations which revealed the presence of Cu_2O and CuO in the XRD analysis also have shown the presence of CuO and Cu^0 in the XPS patterns. The binding energy values $Cu2p_{3/2}$, Mg2p, O1s and C1s along with the Cu/Mg atomic ratios, Cu_s/Cu_p (intensity ratios of the Cu2p satellite peak and Cu2p parent peak) are presented in Table 2. C1s (285.0 eV) is taken as the reference in calibrating the binding energies of the all the other elements viz., Cu, Mg and O. The presence of another minor band of C1s at 289 eV in some of the samples indicates carbon contamination due to CO_3^{2-} species with the exposure of the samples to air. The presence of higher amount CuO species on the surface in these reduced samples may be due to the re-oxidation of Cu^0 on exposure to air. The Cu/Mg ratios suggest the increase in the surface concentration of Cu species with increase in Cu content upto 16 wt.% loading. There after, a decrease of Cu/Mg ratio with Cu loading of 37.3 wt.% and again an increasing trend with loading upto 79.8 wt.% of Cu is seen. This sudden decrease in the Cu/Mg ratio may be due to the dissolution of some Cu species in to bulk with increase in Cu content but a further increase again resulted in surface enrichment of copper species since there is a corresponding decrease of MgO with increase in Cu loading. The trend observed with XPS analysis is however, different from what is observed in our earlier work [15]. The surface enrichment or high Cu/Mg ratios in the samples with the higher loadings of Cu may be mainly due to the presence of CuO species. The increase of Cu_s/Cu_p i.e., the intensity ratio of the satellite peak to the parent peak of Cu $2p_{3/2}$ with increasing Cu content also confirms the presence of more number of CuO species on the catalysts with higher loadings of Cu. The Cu–MgO catalyst with 79.8 wt.% of Cu has a Cu_s/Cu_p value of 0.7660 which is closer to the value observed with the bulk CuO sample (Table 2). The increase of Cu^{2+} or CuO species have been clearly indicated by the increase of intensity of satellite peak of Cu2p at 942.4–943.6 eV in the XPS spectra of the Cu–MgO catalysts. These satellites have been attributed to the shake up transitions by ligand → metal 3d charge transfer which is very characteristic of Cu^{2+} compounds and is not seen in Cu^+ compounds or in metallic Cu because of

Table 2
Binding energy values $Cu2p_{3/2}$, Mg2p, O1s and C1s along with the Cu/Mg atomic ratios, Cu_s/Cu_p (intensity ratios of the Cu2p satellite peak and Cu2p parent peak)

| Catalyst	$Cu2p_{3/2}$ (parent)	$Cu2p_{3/2}$ (satellite)	Cu_s/Cu_p	Mg2p	O1s	C1s	Cu/Mg (atomic ratios)
CuO	933.548	942.232	0.7164	–	529.570, 531.05	284.638, 288.943	–
CM1	933.762	–	–	50.330	531.995	285.40	0.0747
CM2	933.353	–	–	50.027	531.605	285.182	0.1212
CM3	933.804	943.281	0.5820	49.957	531.606	285.177	0.0927
CM4	933.472	942.829	0.4377	49.795	531.427	284.778	0.4252
CM5	933.245	942.742	0.4906	48.910	530.787	284.479, 289.065	0.1058
CM6	934.119	943.653	0.4034	50.458	532.153	285.315	0.1530
CM7	933.528	942.440	0.6203	49.388	531.052	285.251	0.3296
CM8	933.913	943.241	0.7660	50.737	531.990	285.467	0.7178
MgO	–	–	–	49.759	530.356, 531.818	284.743, 289.871	–
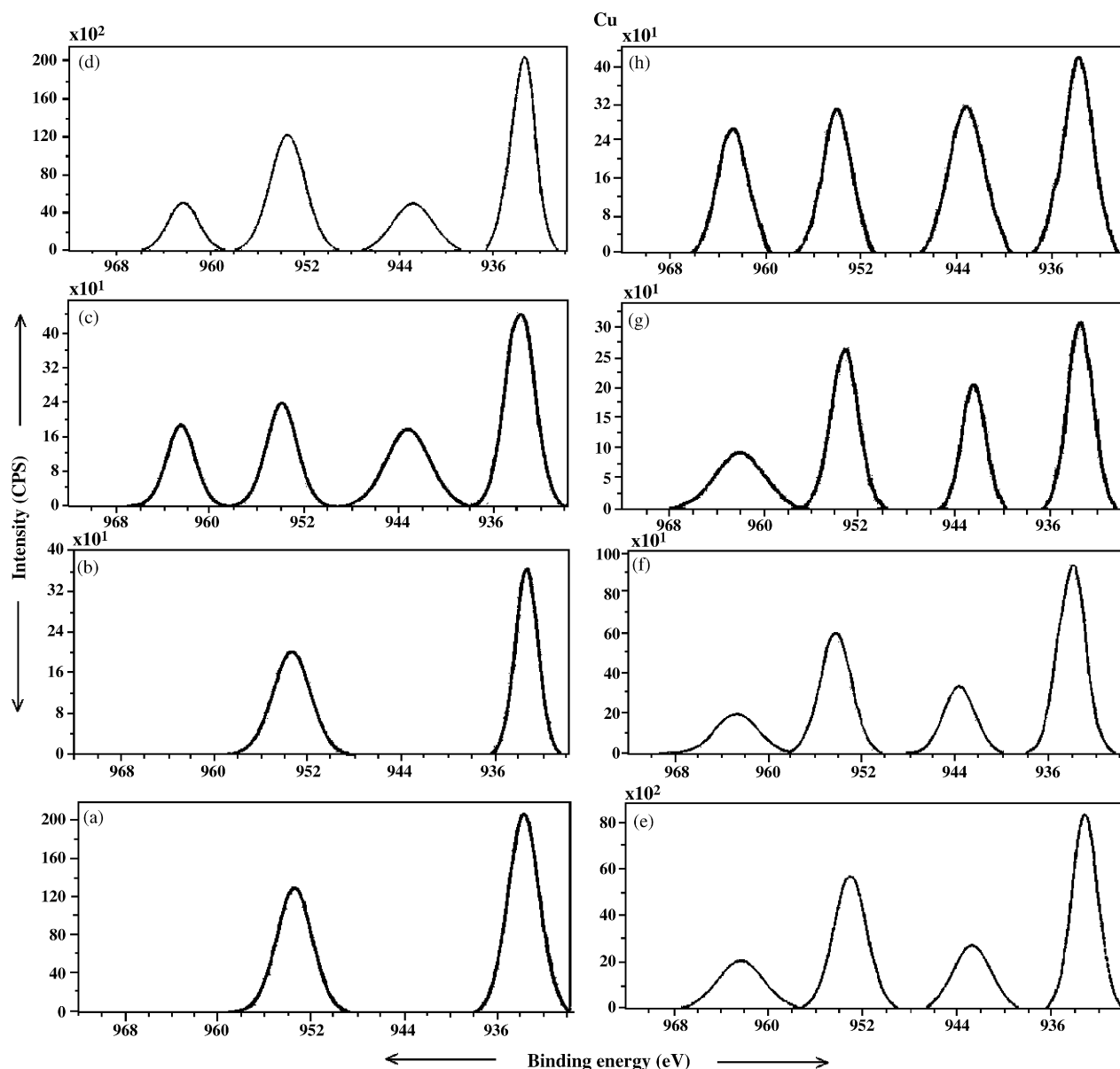
Fig. 2. ESCA patterns of reduced Cu–MgO catalysts: (a) CM1, (b) CM2, (c) CM3, (d) CM4, (e) CM5, (f) CM6, (g) CM7 and (h) CM8.

completely filled 3d shells [18]. In fact, transition metal ions are well reported [19,20] to have unfilled 3d orbital that show well separated satellite peaks in the core level XP spectra due to electron shape-up and the structure of satellite i.e., the peak number, intensity and splitting, reflects the nature of chemical bondings of the transition metal ions. The Cu/Mg ratio is although high with CM4 (16 wt.% Cu), the lower Cu_s/Cu_p in this sample and also CM5 and CM6 samples suggest that the surface enrichment of species viz., Cu^0 or Cu_2O apart from Cu^2 species. Our earlier observations in the hydrogenation of furfural to furfuryl alcohol over Cu–MgO coprecipitated catalyst indicated that the presence of more Cu^0 species in this catalyst to be responsible for its higher activity and selectivity towards the formation of furfuryl alcohol [15].

O1s spectra show the binding energy values in the range of 530.8–532.2 eV for the Cu–MgO catalysts that is characteristic

of metal oxides and is closer to O1s binding energy in MgO. The Mg2p binding values are almost the same in all the catalysts, which shows that there is no variation of surface concentration of MgO with increase in Cu content in the catalysts.

3.3. DTA-TG results

The thermal behaviour of the various Cu–MgO dried samples are studied by DTA analysis in the temperature range of 298–1273 K. Thermal changes accompanied by the corresponding weight recorded are depicted in Fig. 3. The low temperature endotherms in the region 343–473 K showing a weight loss of 2–10% corresponding to weight loss associated with the removal of weakly adsorbed water molecules (physisorbed water) associated with Cu and Mg cations. The lower percentage weight loss with higher Cu content of the samples indicate that the asso-
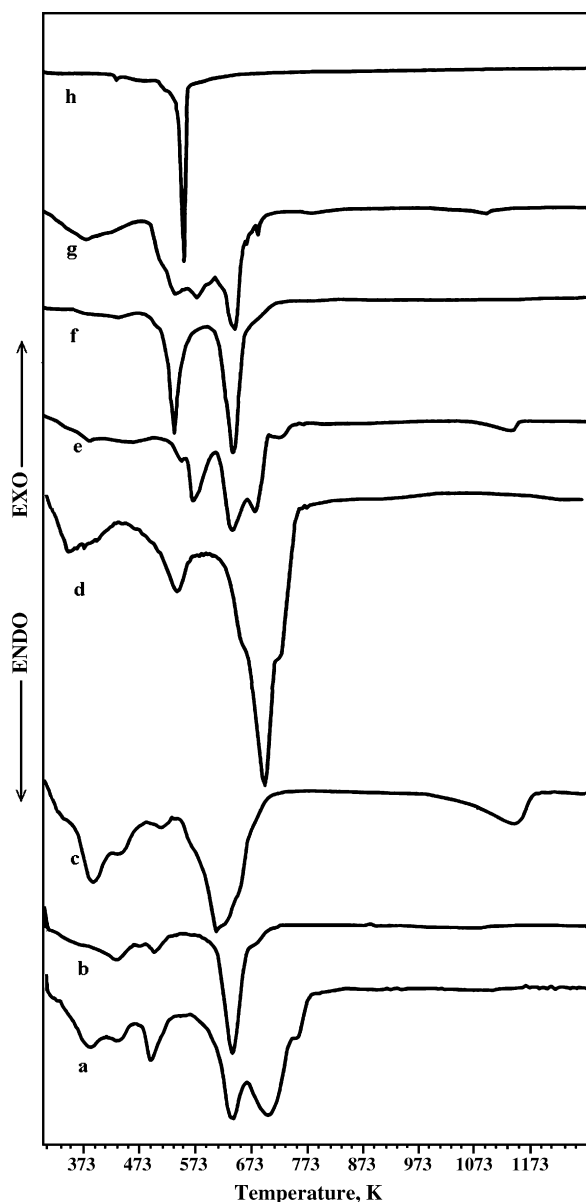
Fig. 3. DTA patterns of Cu–MgO dried catalysts: (a) CM1, (b) CM2, (c) CM3, (d) CM4, (e) CM5, (f) CM6, (g) CM7 and (h) CM8.

ciation of such weakly bound water is higher with Mg cations or the affinity of Mg cations towards the water molecules is higher compared to Cu cations. The next major transitions are observed in the region of 493–633 K correspondingly showing a percentage weight loss of 10–48% with samples of higher Cu concentrations losing more weight in this region and in fact, the sample CM8 showed no further significant loss in weight above 623 K upto 1273 K. These transitions or endotherms can be attributed to the dehydration/dehydroxylation or decarboxylation process corresponding to the loss of hydroxyl groups or CO_3^{2-} of Cu and Mg. The two main endotherms of this process seen in the range of 493–533 K and ~633 K can be ascribed to the loss of hydroxyl groups of Cu and Mg, respectively attributed to the decomposition of carbonates of their corresponding oxides. The individual DTA patterns of dried samples of simple CuO and MgO (prepared under similar conditions as the Cu–MgO

coprecipitated catalysts) showed endotherms at 493–533 K and ~633 K, respectively (the patterns of which are not presented here). These transitions occur in two stages in certain samples viz., CM1, CM2 and CM4 with shoulders appearing on the high temperature side. The endotherm observed at temperatures above 673 K with a shoulder around 723–753 K can be associated to the dehydroxylation and decarboxylation processes taking place with the probable presence of Cu and Mg hydroxyl carbonates, owing to K_2CO_3 used in the preparation of Cu–MgO samples as a precipitating agent. The transitions that occur in the range of 673–773 K have been attributed by various authors to the removal of CO_2 associated with Cu containing samples [21–23]. The presence of IR bands in the region of 1350–1380, 850–690, 670–690 cm^{-1} arising from carbonate anions (not shown in the figure) further confirms these transitions observed in the DTA patterns. The minor transition (endotherm) observed at a high temp of 1073–1123 K in the CM2 and CM4 samples can be attributed to the partial transformation of CuO to Cu_2O, which is even in the presence of oxygen atmosphere [21–25]. In all other samples except for CM8 also there is a slight weight loss observed above 1073 K, although no endotherm at such position is noticed which suggests that the $CuO \rightarrow Cu_2O$ transition might have taken place but not to a significant extent. The typical pattern of CM8 showing only a single sharp endothermic peak ~548 K suggests that the dehydroxylation process owing to the loss of hydroxyls on Cu is more significant and since the contribution from the hydroxyls on Mg is very less there may be an overlap of the two taking place giving a single peak.

3.4. Activity measurement

A successful demonstration of non-chromium containing Cu–MgO as a highly efficient catalyst in the vapor phase hydrogenation of FAL to FOL has been reported earlier by us [15]. The advantage of a Cu–MgO catalyst prepared by coprecipitation method over the other methods is clearly shown. The coprecipitated catalyst yielded FOL more selectively on account of higher number of Cu^0 metal species which are in interaction with the oxygen vacancies of MgO and with suitable Cu^0 metal particle size. The emphasis is on the development of a non-chromium containing and more efficient catalyst for the synthesis of FOL. The present report is a further study to see the effect of Cu loading and reaction temperature on the furfural hydrogenation activity over Cu–MgO coprecipitated catalyst.

Scheme 1 shows an overall view of the reaction pathways and possible formation of various products in the hydrogenation of FAL to FOL. The other products viz., 2-methyl furan (MF), furan (F), tetrahydrofuran (THF) and tetrahydrofurfuryl alcohol (THFOL) are formed as minor products or in trace amounts. The selectivity to FOL is reported to be governed mainly by (a) metal-support interactions, (b) electronic and steric influence of the support, (c) morphology of the metal particles, (d) selective poisoning, (e) influence and nature of second metal, (f) effect of pressure and (g) steric effects of substituents at the conjugated double bond [26].

Fig. 4 depicts the effect of reaction temperature on the catalytic activity of CM4 (Cu–MgO coprecipitated catalyst with

Scheme 1. The plausible reactions in the hydrogenation of furfural.
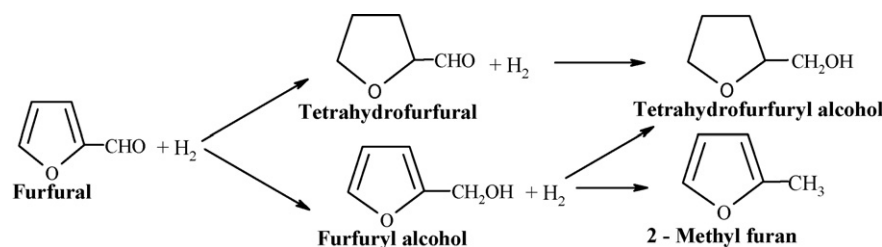
16 wt.%. of Cu) at a H$_2$: furfural molar ratio = 2.5 and furfural feed rate of 1.2 ml h^{-1}. There is no significant variation observed in the percentage conversion of FAL with rise in temperature above 453 K. But, a fall in the selectivity to the desired product FOL can be seen with increase in temperature from 453 K on account of formation of other products viz., MF, THFOL, THF, etc. Some authors report similar observations, over other Cu-based catalysts i.e., Pt-based and Ni-based catalysts [5,27–29]. However, further hydrogenation is also found to take place along with FOL formation [29,30]. The advantage of copper-based catalysts, thus, seems to be to achieve selective hydrogenation of the C=O bond while keeping the C=C bond in the furan ring intact.

The formation of other products responsible for the fall in the selectivity to FOL at higher temperatures can be attributed to the activation of C=C bond in the furan nucleus at these temperatures giving rise to the further hydrogenation products. At lower temperatures it seems that only C=O bond is activated selectively to yield FOL. Thermodynamically C=C bond hydrogenation is more favored over C=O bond hydrogenation [31]. Selective activation of C=O group has been successfully carried out catalytically over various Cu-based and other Pt, Ni-catalysts [26].

In absence of any steric constraints induced by substituents, hydrogenation of C=C group is preferred over the hydrogenation of C=O group in the hydrogenation of α,β-unsaturated aldehydes [26]. The competitive adsorption of the olefinic and the carbonylic group plays an essential role in determining the selectivities of the products, whether it is to an unsaturated alcohol or a saturated aldehyde. The difference in reactivity has been related to the adsorption modes of the olefinic bond on the one side and of the aldehydic (ketonic) bond on the other side [32]. The steric hinderances of the olefinic group seem to enhance the adsorption through the carbonyl group. Ponec et al. reported that the choice of metal influences the activity and selectivity which could be manipulated by the use of a promoter an alkali metal ion, transition metal compounds or a non-transition element viz., Sn, Ge and Ga [33]. They further state that the relative accessibility and the binding strength of C=C and C=O groups, with the addition of hydrogen to C=C bonds of the furan ring is sterically hindered, and thus selective activation of the carbonyl group can be achieved to yield furfuryl alcohol [34].

The effect of Cu loading on furfural hydrogenation activity of Cu–MgO catalyst has been shown in Fig. 5. All the catalysts of Cu–MgO have shown much higher activity compared to bulk CuO catalysts. It can be observed from the graph that the conversion of FAL and selectivity to FOL (correspondingly yield of FOL) enhanced with increase in Cu content upto ∼16 wt.% (CM4). A drop in conversion of FAL is observed over CM5 and CM6 and there is not much variation of selectivity to FOL seen over these catalysts. A further increase in Cu content resulted
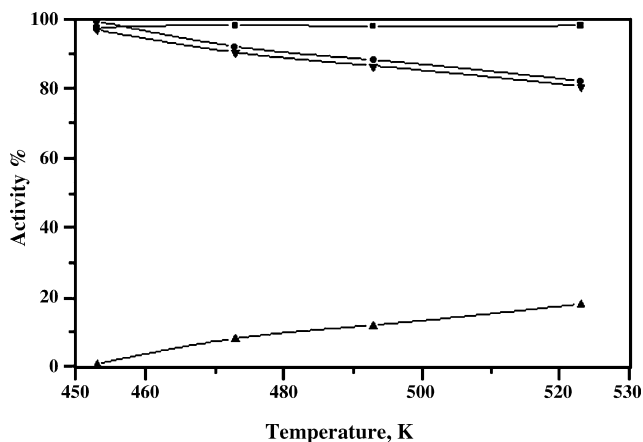

Fig. 4. Effect of reaction temperature on the conversion of furfural over Cu–MgO coprecipitated catalyst at H$_2$/furfural molar ratio = 2.5 and GHSV = 0.05 mol h^{-1} g cat^{-1}: (■) conversion of FAL, (●) selectivity of FOL, (▲) selectivity of others and (▼) yield of FOL.

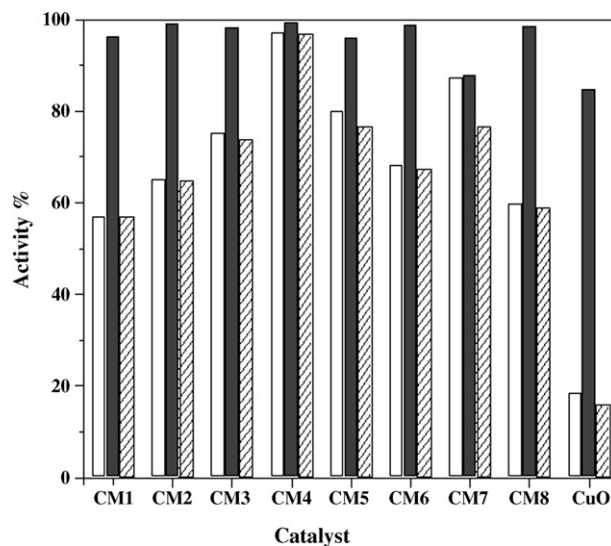Fig. 5. Effect of Cu loading on the furfural conversion at H$_2$/furfural molar ratio = 2.5, reaction temperature = 453 K and GHSV = 0.05 mol h^{-1} g cat^{-1} over Cu–MgO catalysts: (□) conversion of FAL, (■) selectivity of FOL and (▨) yield of FOL (remaining percentage selectivity corresponds to 2MF, Furan and THFA).

in the loss of selectivity to FOL as well as conversion levels of FAL, with the catalysts behaviour being similar to that of bulk CuO at these higher loadings of copper. The XPS results support these observations. The increase in CuO species over the surface is evidenced with an increase in the intensity ratios of Cu_s/Cu_p from XPS and rise in the intensity of CuO 'd' lines from XRD is seen with higher Cu contents in the catalyst. Thus, it can be opined that more the Cu^0 species or lesser the CuO species, higher is the activity shown by the catalysts towards selective formation of FOL from the hydrogenation of FAL. A controversy still exists over the type of copper species which act as active sites for the type of hydrogenation reactions. Some authors suggest only Cu^+ species and some others opine both Cu^+ and Cu^0 are the active sites for the hydrogenation reactions over Cu-based catalysts [5,10,35,36]. A clear illustration of a Langmuir–Hinshelwood model invoking either one type of site with competitive adsorption between furfural and hydrogen or two types of sites i.e., one for each reactant has been shown by Rao et al. in the hydrogenation of furfural over copper chromite catalyst [10]. They further suggested a simple bimolecular surface reaction as a rate-determining step by correlating Cu^+ sites with activity and proposed that presence of both Cu^+ and Cu^0 species to be required for optimum performance. The activity results and the characteristics observed from XRD and XPS analyze in the present study also clearly indicate the necessity of both the species of Cu^+ and Cu^0 for the hydrogenation of FAL to FOL. Since, the Cu–MgO catalysts that contain these two species have shown superior activity and the ones with higher Cu content having more Cu^{2+} species are found to be less active for this reaction. The turnover frequency (TOF) of furfural conversion against Cu loading is shown in Fig. 6. The turnover frequency is defined as number of furfural molecules converted per second per surface Cu site. The number of surface Cu-sites is obtained from N_2O pulse chemisorption technique assuming a stoichiometry of 1:2 between N_2O and Cu. The experimental
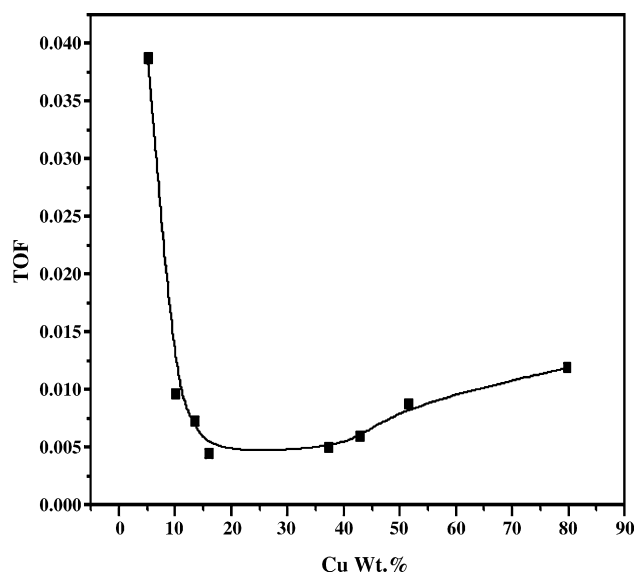
details are shown in our previous publication [16]. From Fig. 6, it is clear that the turnover frequency (TOF) is higher in the catalysts containing lower Cu composition. However, lack of required number smaller Cu particles and the absence of Cu^+ species make these catalysts inferior in furfural hydrogenation. The XPS data of Cu_s/Cu_p ratios (Table 2) suggest that although the catalysts CM4 (16 wt.%) and CM7 (52 wt.%) vary to a great extent interms of Cu contents, they seem to show same Cu_s/Cu_p ratios (Table 2), which suggest a surface enrichment of copper (Cu^0/Cu^+) species in CM4 and CM7. However, probable agglomerization of copper particles as CuO in CM7 responsible for its low activity compared to that of CM4.

4. Conclusions

The hydrogenation studies of furfural to furfuryl alcohol over Cu–MgO coprecipitated catalyst indicated that the presence of more number Cu^0/Cu^+ species on the catalyst surface which are therefore is responsible for the high activity and the selectivity towards furfuryl alcohol. The activity results and the XPS characteristics observed clearly indicate the necessity of both the Cu^+ and Cu^0 species for the hydrogenation of FAL to FOL. This is indicated from the higher Cu/Mg atomic ratio and a lower Cu_s/Cu_p ratio observed with CM4 (16 wt.% Cu) from XPS analysis showing the highest activity and selectivity towards the desired product at 453 K.

Acknowledgements

Fig. 6. Turnover frequency (TOF) of furfural conversion against Cu loading in Cu–MgO coprecipitated catalysts.

References

[1] W.J. Mickillip, in: B. Elvers, S. Hawkins, M. Ravenscroft, J.F. Rounsaville, G. Schulz (Eds.), Ullmann's Encyclopedia of Industrial Chemistry (5th completely revised edition), vol. A12, VCH Verlagasgesellschaft mbH, Federal Republic of Germany, 1989, p. 125.
[2] K. Othmer, in: G.J. Bushey, C.I. Eastman, A. Klingsberg, L. Spiro (Eds.), Encyclopedia of Chemical Technology, Sons Inc., USA, 1980, p. 510.
[3] K. Bauer, D. Garbe, Common Fragrance and Flavor Materials, VCH Publishers, Kyoto, Japan, 1985.
[4] M.S. Li, W.Z. Ma, Hebai Ind. (1999) 6.
[5] R.S. Rao, R.T.K. Baker, M. Vannice, Catal. Lett. 60 (1999) 51.
[6] B.J. Liu, L.H. Lu, B.C. Wang, T.X. Cai, K. Iwatani, Appl. Catal. A: Gen. 171 (1998) 117.
[7] De Thomas, US patent 4, 153 (1979) 578.
[8] H.S. Luo, H.X. Li, L. Zhuang, Chem. Lett. (2001) 138.
[9] Z. Huang, L. Qiu, Shiyou Huagong, 21 (1992) 35.
[10] R.S. Rao, A. Dandekar, R.T.K. Baker, M.A. Vannice, J. Catal. 171 (1997) 406.
[11] S.P. Lee, Y.W. Chen, Ind. Eng. Chem. Res. 38 (1999) 2548.
[12] H. Luo, H. Li, L. Zhuang, Chem. Lett. 5 (2001) 404.
[13] J. Nowicki, Z. Maciejewski, Przem. Chem. 76 (1997) 53.
[14] M.J. Burk, T. Harper, P. Gregory, J.R. Lee, Ch. Kalberg, Tetrahedron Lett. 35 (1994) 4963.
[15] B.M. Nagaraja, V. Siva Kumar, V. Shasikala, A.H. Padmasri, B. Sreedhar, B. David Raju, K.S. Rama Rao, Catal. Comm. 4 (2003) 287.

[16] B.M. Nagaraja, V. Siva Kumar, V. Shashikala, A.H. Padmasri, S. Sreevard-han Reddy, B. David Raju, K.S. Rama Rao, J. Mol. Catal. A 223 (2004) 339.

[17] A.F. Carley, M.K. Rajumon, M.W. Robetrs, J. Solid State Chem. 106 (1993) 156.

[18] K.S. Kim, J. Electron Spectrosc. Relat. Phenom. 3 (1974) 217.

[19] D.C. Frost, A. Ishitani, C.A. McDowell, Mol. Phys. 24 (1972) 861.

[20] T.A. Carlson, Photoelectron and Auger Spectroscopy, Plenum Press, New York, 1975.

[21] V. Rives, A. Dubey, S. Kannan, Phys. Chem. Chem. Phys. 2 (2001) 4826.

[22] B. Montanari, A. Vaccari, M. Gazzano, P. Kaβner, H. Papp, R. Dziembaj, W. Makowski, T. Lojenski, R. Dziembaj, Appl. Catal. B: Environ. 35 (2002) 195.

[23] A. Alejandre, F. Medina, X. Rodriguez, P. Salagre, J.E. Sueiras, J. Catal. 188 (1999) 311.

[24] L. Chmielarz, P. Ku'strowski, A. Rafalska-Lasocha, D. Majda, R. Dziembaj, Appl. Catal. B: Environ. 35 (2002) 195.

[25] F. Kovanda, K. Tiratova, J. Rames, D. Kolonsek, Appl. Clay Sci. 18 (2001) 71.

[26] P. Claus, Topics Catal. 5 (1998) 51.

[27] J.G.M. Bremner, R.K.F. Keeys, J. Chem. Soc. (1947) 1068.

[28] M.S. Borts, N.D. Gil'chenok, V.M. Ignate'er, G.S. Gurevich, Zh. Prikl. Khim. 59 (1986) 126.

[29] G. Seo, H. Chon, J. Catal. 67 (1981) 424.

[30] A. Kaufman, J.C. Adams, J. Am. Chem. Soc. 45 (1923) 3029.

[31] M.A. Vannice, B. Sen, J. Catal. 115 (1989) 65.

[32] T. Birchem, C.M. Pradier, Y. Berthier, G. Cordier, J. Catal. 146 (1994) 503.

[33] T.B.L.W. Marinelli, S. Nabuurs, V. Ponec, J. Catal. 151 (1995) 431.

[34] T.B.L.W. Marinelli, V. Ponec, C.G. Raab, J.A. Lercher, in: M. Guisnet, J. Barbier, J. Barrault, C. Bouchoule, D. Duprez, G. Perot, C. Montassier (Eds.), Heterogeneous Catalysis and Fine Chemicals III, vol. 78, Elsevier, Amsterdam, 1993, p. 195.

[35] F.M. Capece, V.D. Castro, C. Furlani, C. Mattogno, C. Fragale, M. Gargano, M. Rossi, J. Elec. Spec. Relat. Phenom. 27 (1982) 119.

[36] E. Nishimura, Y. Inuoue, I. Yasumori, Bull. Chem. Soc. Jpn. 48 (1975) 803.